လp

CIRCULAR ENERGY VORTEX IN THE NEAR FIELD
OF A DIRECTIONAL ANTENNA

F. Landstorfer, H. Heinke and
G. Niedermair

IN THE NEAR FIELD OF A DIRECTIONAL
ANTENNA (Scientific Translation Service)
16 p HC $3.00   CSCL 17B
/S

N74-14898

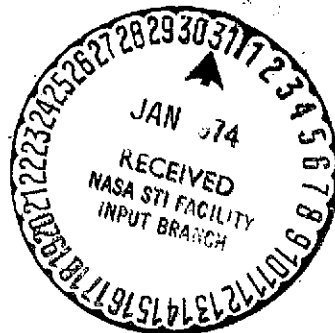   Unclas
                                        G3/07   27356

CIRCULAR ENERGY VORTEX IN THE NEAR FIELD
OF A DIRECTIONAL ANTENNA *

Friedrich Landstorfer, Hans Meinke
and Günter Niedermair

1. INTRODUCTION

In [1] it was shown that additional information on the
behavior of electromagnetic waves can be obtained in complicated
cases by considering the energy flow and the energy streamlines.
The vortex regions influence the energy flow in a particular way.
In these regions, the energy rotates in closed regions around
an axis and therefore they represent an important obstacle for the
wave propagation. Up to the present we had only studied such
vortex zones in waveguides [2]. We have now also found them in
infinite space in the vicinity of directional antennas. The clear
relationships between the far field directional diagram and the
near field vortex zones show that these vortices play a
significant role in the establishment of the directional effect
for many directional antennas. In this paper we will restrict
ourselves to the example of a directional antenna for which the
vortex was first discovered. In a second paper we will then
describe other examples and will discuss the connection between
the vortices and the directional effect in more detail.

** Numbers in the margin indicate pagination of original foreign
   text.

Up to the present, vortices have only been calculated or measured in certain cross section planes [2,3]. It is remarkable that for the first time we were able to measure a spatial vortex formation which has a ring shape and closed central line.

2. DIRECTIONAL ANTENNA WITH HEMISPHERICAL DIELECTRIC

Figure 1 shows the antenna for which the near field was investigated. It is an asymmetric antenna with a coaxial feed on a conducting base plane. The asymmetric shape was selected in order to be able to install the generator and the measurement apparatus below the conducting plane without disturbing the antenna field. No problems occur in practical applications if the conducting plane is omitted and if the structure is complemented in a symmetric way by installing a symmetric antenna.

Originally we intended to build simple microwave directional antennas using dielectric directional members. We started out with a dielectric hemisphere shown in Figure 1. If one wishes to produce the directional effect with relatively small dielectric members, it is necessary to excite the wavefield directly inside of the dielectric. The simplest technological solution and the one which functioned the best was an arrangement in which a coaxially fed area conductor was the exciting radiator and was directly glued to the surface of the dielectric member. A radiator shape was found which had good matching properties to the feed cable over a very large frequency range. The hemisphere diameter was 27 cm which resulted in a measurement range between 400 and 1250 MHz.

Since it is not possible to analyze such an antenna theoretically, we measured the near field using probes which were already described in [4] and [5]. We measure the distribution of the
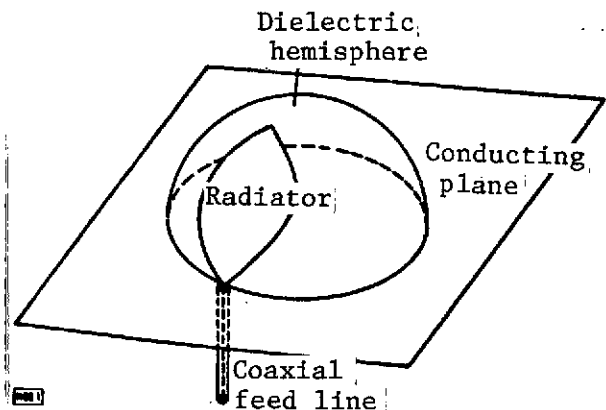
2

Figure 1. Dielectric hemisphere above a conducting plane with a radiator having a coaxial feed
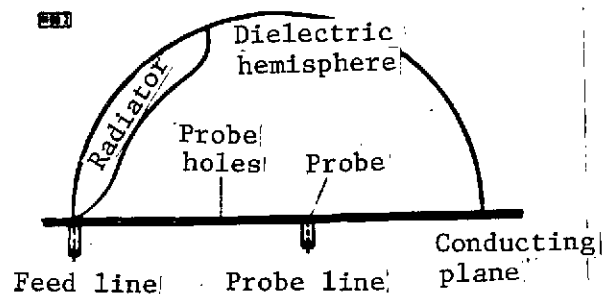

Figure 2. Longitudinal cross section with bore holes in the base plane

field on the surface of the conducting base plane. We determine the amplitude and the phase by drilling many holes through the plane according to Figure 2. The field strength is then measured with probes inserted in these holes. The electrical field strength is measured with electrical probes (extended inner conductor of the coaxial probe line). The magnetic field strength is measured with magnetic probes (electrically shielded loops at the end of the probe line). It is tangential to the conducting plane and is elliptically polarized. In contrast to   /538 our earlier measurements, we also wanted to measure below the dielectric hemisphere without having to drill the dielectric. This meant that the probes could not stick out of the surface of the conducting plane. This is why we used conical holes, as shown in Figure 3 together with an electrical probe. All probes are within the conical hole. All holes are exactly the same. The snapping springs in the probe holders insure that the probe has the same position in all the bore holes. The accuracy is important here, so that the individual measurements can be quanti- tatively compared. Three hundred bore holes resulted in a sufficiently accurate result. Only the right half of the field was measured because the field is symmetric with respect to the
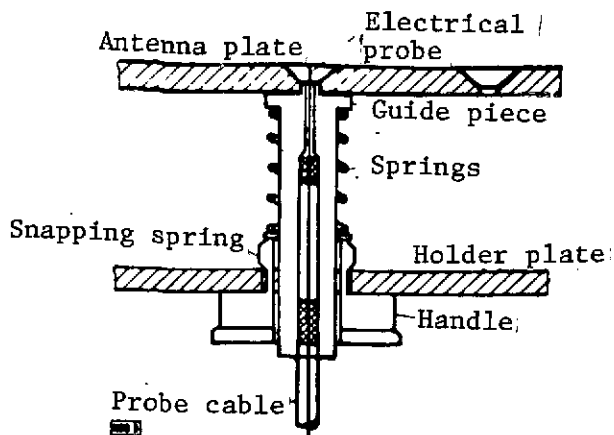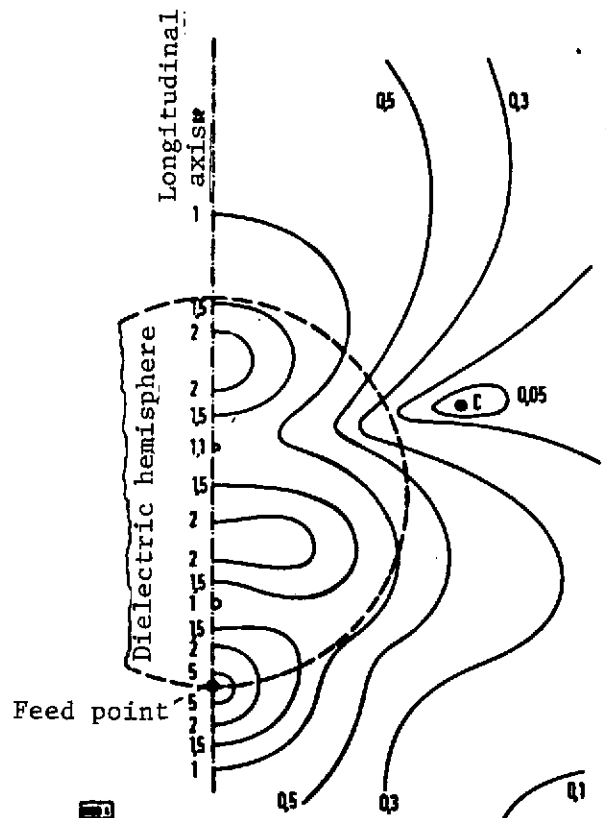
Figure 3. Electrical probe in the tube hole.

Figure 4. Lines of constant amplitude of the electrical field strength on the basic plane; dashed line: dielectric hemisphere.

longitudinal axis (principal radiation direction), as shown in Figure 4. The calibration procedures for the installation and the evaluation of measurements are described in [7].

3. ENERGY VORTICES IN THE NEAR FIELD

The measurement results for the electrical normal field strength along a conducting plane is best described by lines of constant amplitude (Figure 4) and by lines of constant phase (Figure 5) along the conducting base plane. These figures and the following figures show the dielectric hemisphere as a dashed circle. The coaxial feed point is represented by a black dot. Figures 4 and 5 give a variation of the amplitudes and phases of the electrical field strength along the longitudinal axis. This shows that there is a wave in the interior of the dielectric hemisphere which starts at the radiator, and part of this wave is reflected at the surface of the hemisphere. Within the hemisphere, the first wave and the reflected wave superimpose along
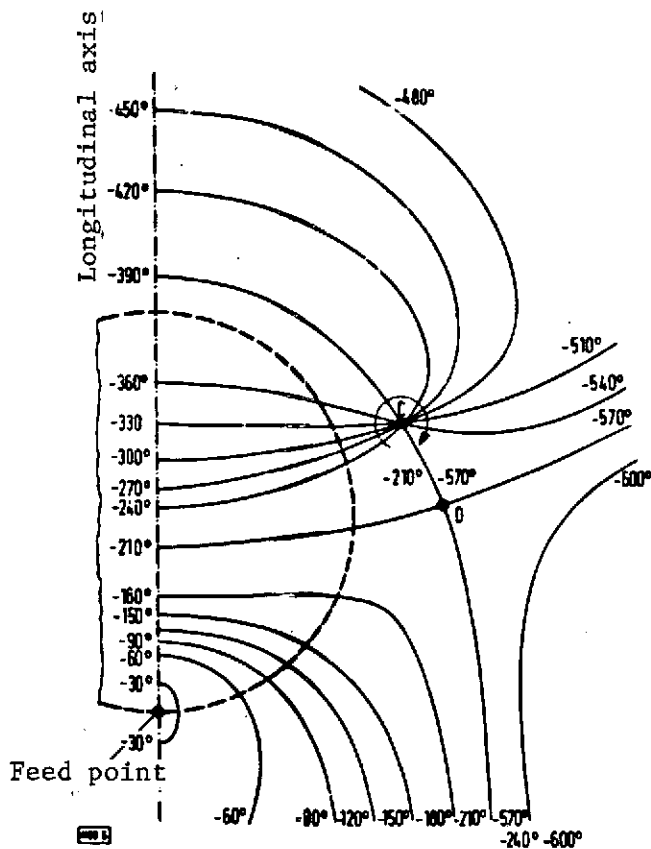
Figure 5. Lines of constant
phase of electrical field
strength on the base plane;
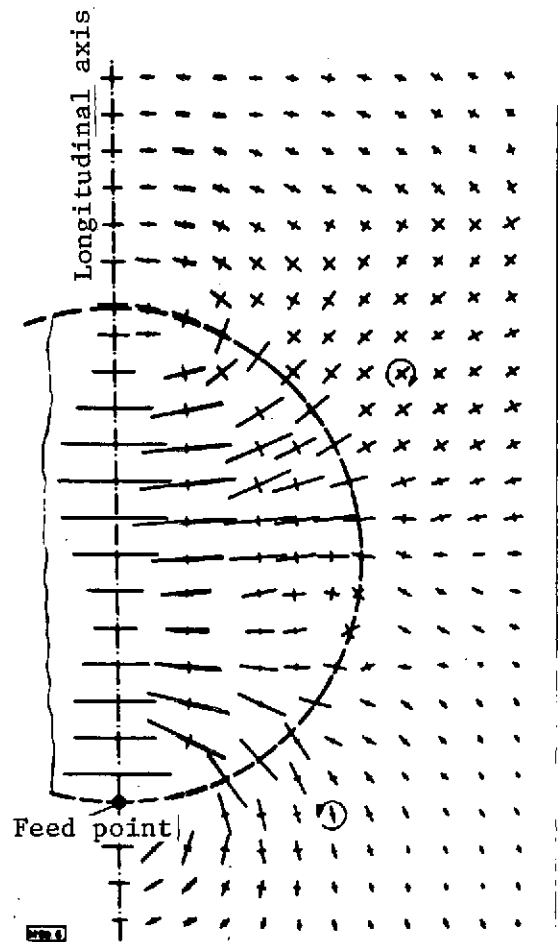vortex center C; stagnation
point D

Figure 6. Polarization ellip-
ses of magnetic field strength
on the base plane

the longitudinal axis, similar to what happens in a mismatched
line. These internal reflections of the hemisphere are responsible
for the frequency dependence of the antenna behavior. In general,
the wave state in the interior of the directional member is
easily recognized for such dielectric directional members, having
arbitrary shape. The point C of the field is of particular
interest. At point C the electrical field strength becomes zero
as shown in Figure 4, and many phase lines intersect there accord-
ing to Figure 5. If one moves around the point C in Figure 5 in

the direction shown, then the phase changes by 360° during each
revolution. Such a field variation is characteristic for an
energy vortex [6]. Two distinct lines having equal phase
intersect at point B in Figure 5, which later on will be shown
to be the stagnation point of energy.

The energy vortex becomes clearly visible if the energy
motion is considered. For this it is necessary to also consider
the magnetic field. From this it is possible to determine the
time-averaged Poynting vector, also called the vector of energy
flux density [1]. The tangential magnetic field strength H along
the conducting base plane is elliptically polarized. By rotating
the loop of the magnetic probe, it is possible to measure the
polarization ellipse. Figure 6 shows the position and size of
the axes of the polarization ellipse for many measured points.
The polarization is linear along the longitudinal axes of the
wave field. In certain regions, the polarization ellipses
run in the clockwise direction and in others, they run in the
counter clockwise direction.

The time averaged Poynting vector, i.e. the time average
energy flux density direction and magnitude, is tangential to
the conducting base plane, that is, perpendicular to the electri-
cal field strength vector. In this paper, with an elliptically
polarized magnetic field, it is the vector product of the
electrical field strength and the magnetic field strength H of
the polarization ellipse, which has the same phase as the
electrical field strength E at the same location [1]. The
direction of the time average energy flux is therefore everywhere
perpendicular to the component of the magnetic vector which has
the same phase as the vector E. This vector with the same phase
has almost the direction of lines of constant E-phase in the
conducting plane (Figure 5). Therefore, the energy flux density

vector is approximately perpendicular to the lines of constant phase. This means that the phase relationship of the vector H must be known in the polarization ellipse. For this purpose, one measures the following:

1. The direction of rotation of the polarization ellipse. As indicated in Figure 6, there are ellipses which run in the clockwise direction as well as ellipses which run in the counterclockwise direction. Each occur in connection regions.

2. The phase angle of the vector H for the semimajor axis of each ellipse with respect to the reference phase indicated by the measurement apparatus.

3. The phase difference between the reference phase when E is measured and the reference phase when H is measured. The latter is obtained by calibrating the phase indication of the E probe and the H probe at a bore hole for a homogeneous line having a standing wave, in which the phase difference between E and H is exactly $\pi/2$.

Figure 7 shows many such energy flux vectors corresponding to the vectors E and H given in Figures 4 to 6. One can recognize the principal directions of the time average energy flux and the rotation of the energy around the point C. The energy streamlines [1] give a clearer indication of this. Everywhere they have the direction of the vector of time average energy flux density in Figure 7. They are shown in Figure 8. Figure 8 shows both sides of the dielectric sphere. On the left side there is the vortex center C' symmetric with respect to C. Also the stagnation point D' is indicated which is symmetric with respect to D. There are three groups of field lines. One group starts at the feed point S and passes through the space between
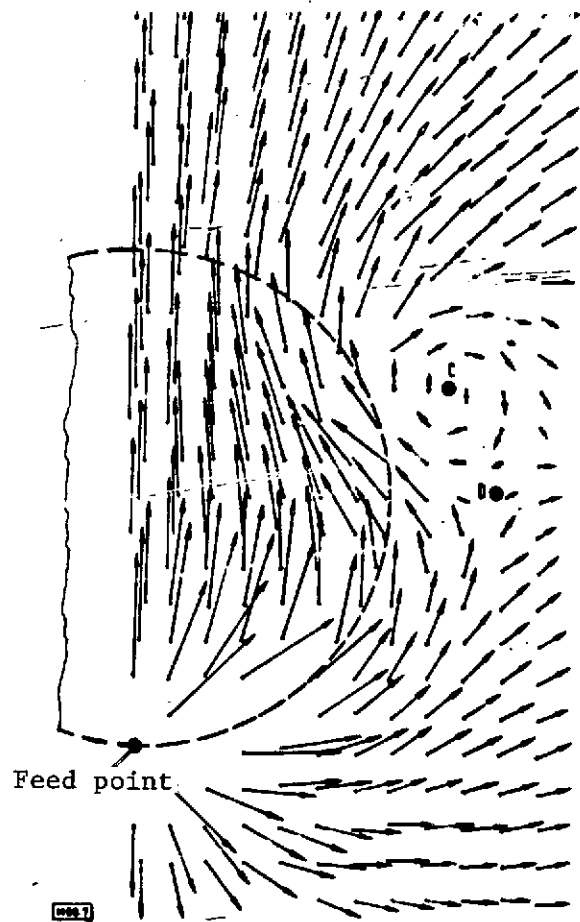
7

Figure 7. Vectors of the time-average energy flux density on the base plane
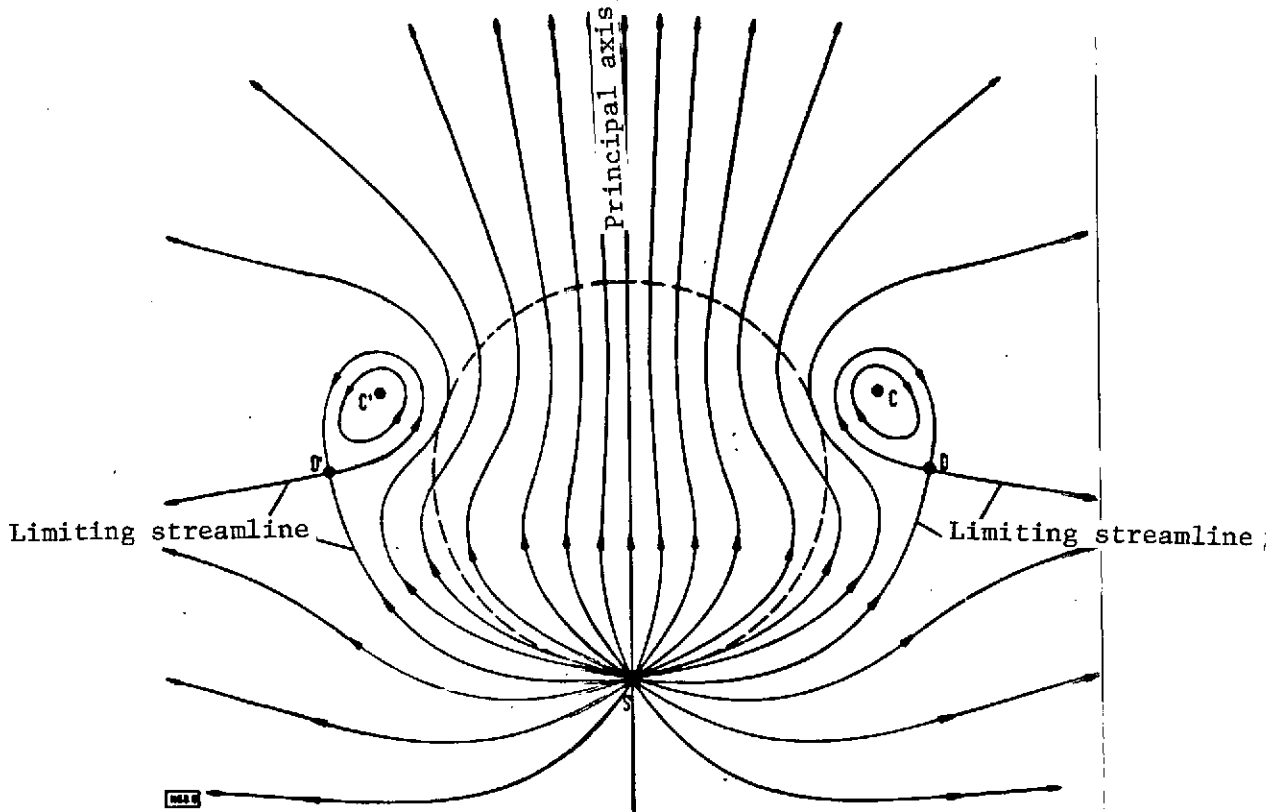
Figure 8. Streamlines of the time average energy flux along the base plane.

C and C'. The second group starts at the feed point and remains outside of the region limited by C and C'. A certain part of the energy rotates around the points C and C' and forms the energy vortex. Figure 8 shows the mentioned groups of streamlines separated by two limiting lines, which themselves intersect perpendicularly at point D and D', respectively, and which surround the vortex center. The energy flux density is zero at the stagnation point D and D' because E and H have the phase difference $\pi/2$ there [3]. The energy flux density is zero at the vortex center because E = O. Part of the limiting stream-lines which are shown to originate at point D (or D') and which return to D, surround a vortex zone which itself is closed.

It is emphasized that this measurement is limited by its accuracy and can therefore not describe all the processes in detail. This is particularly true in those regions in which the field strengths are very small. This is why the variation of the limiting streamline can only be represented with a limited accuracy here. In future work we will describe the details of energy migration in the vicinity of the limiting streamline based on very exact calculations obtained with Yagi antennas which can be calculated.

The limiting streamline between the feed point S and the stagnation point D divides the energy flux shown in Figure 8 into two parts. The energy flux which emerges above this line from the feed point S represents the principal radiation of the directional antenna. It can clearly be seen how this energy flux is compressed by the vortex and is deflected in the forward direction. A shade zone with a small energy density develops | behind each vortex along the limiting streamline which starts at D and goes to infinity. The energy flux which emerges below the limiting streamline from the feed point S represents the side radiation of the directional antenna. Figure 9 shows the / 540 horizontal far field directional characteristic diagram. It can clearly be seen that the shade zone behind the vortex produces a minimum in the field strength of the far field. The part of the limiting streamline which goes from point D to infinity in Figure 8 becomes a straight line asymptotically, which has the direction of the field strength minimum. In a future paper we will show that such vortex zones are considerably involved in the directional characteristics, even for other directional antennas.

Figure 10 shows the greater neighborhood of the antenna and shows the line of constant phase and the limiting streamline which starts at D. This clearly indicates the transition between the

near field zone and the far field. The phase lines which meet each other to both sides of the limiting streamline have a phase difference of 360°.

4. EXPERIMENTAL VERIFICATION OF A VORTEX RING

It was possible to demonstrate the existence of the vortex only along the conducting base plane using the measurement methods described above. However, the vortex has three-dimensional character. We believe that the vortex has a ring shape formation which connects the two vortex centers. We proved the existence of a ring shaped characteristic central line by performing the following experiment.

According to Figure 12, the electrical measurement probe is placed at the vortex center C. The probe then does not have any output voltage. The probe conductor is extended by 1 cm so that it penetrates into the space above the base plane. The probe then indicates a small output voltage. The probe connection is bent until the initial voltage is zero again. We then extend the probe again by one cm and bend the extension piece until again the output voltage is zero.   By extending the probe in small incre-   /541
ments and bending each extension (keeping the previously shaped piece in the same shape), one obtains a curved probe with a long length as shown in Figure 12, which does not result in any output voltage at the probe cable. This means that along this curve there is no component of electrical field strength. In this way one obtains the entire course of the central line as shown in Figure 11.

We discovered an interesting property of the curve measured in this way by carrying out the following experiment: a copper wire having the shape of the measured curve was connected with a conductor to the base plane at points C and C' as shown in Figure 11.
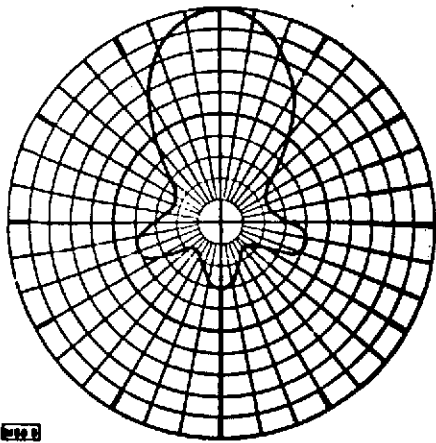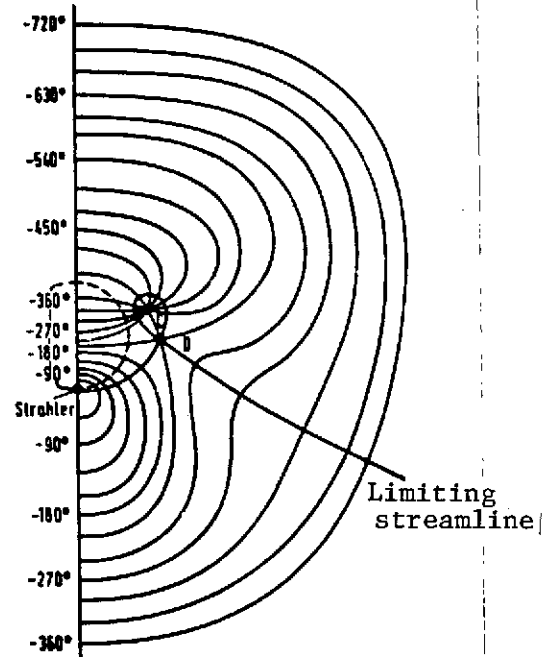
11

Figure 9. Horizontal
far field diagram

Figure 10. Lines of constant
phase of electrical field
strength and the limiting field
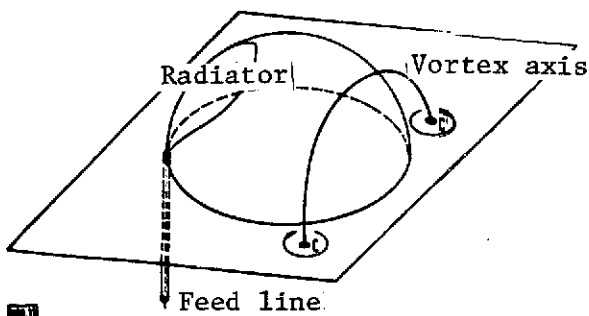line over a larger region.

-720°
-630°
-540°
-450°
-360°
-270°
-180°
-90°
Strahler
-90°
-180°
-270°
-360°

Limiting
streamline

Radiator

Vortex axis

Feed line

Figure 11. Central line
in front of the dielectric
hemisphere
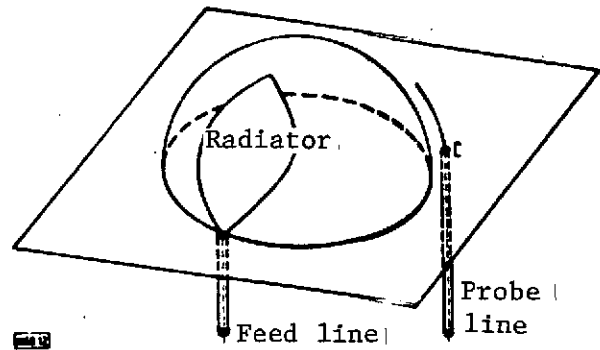
Radiator

Feed line

Probe
line

Figure 12. Measurement of the
central line with a curved
probe

By measuring the radiation impedance and the far field directional diagram, we found that such a wire neither influences the impedance nor the directional diagram of the antenna. This means that it lies along a neutral line for the wave field. If then this wire is bent somewhat, it influences the wave field in a noticeable way. Along the central line it is possible to penetrate into the wave field with long probes without disturbing the field. This means that it is possible to develop other measurement methods for wave fields. A reception antenna can also be installed along the central line which is completely uncoupled from the radiator which transmits energy.

According to Figure 10, such a vortex zone has the effect of a nozzle which pulls the energy flux from the radiator to itself and then blows it out in the forward direction in concentrated form. There is a relationship between the area of the vortex ring and the effective area of the antenna. In such cases, the concept of the effective area would also have meaning for transmission antennas.

REFERENCES

1. Landstorfer, H., H. Liska, H. Meinke and B. Müller. Energy Flow in Electromagnetic Wave Fields. Nachrichtentechn. Vol. 25, No. 5, 1972, pp. 225-231.

2. Liska, H. and H. Meinke. Experimental Verification of the Two Elementary Types of Energy Vortices in Wave Fields. Nachrichtentechn. Vol. 23, 1970, pp. 445-448.

3. Hönl, H., A. W. Maue, and K. Westpfahl. Theorie der Beugung Handbuch der Physik (Theory of Refraction. Handbook of Physics.) Springer-Verlag, Vol. 25/1, Berlin, 1961, pp. 410 and 411.

4. Meinke, H. Scimitar Antennas. Nachrichtentechn. Vol. 20, 1967, pp. 693 to 699.

5. Liska, H. Meinke and C. Mohr. Wave Separation from a Wide Band Cone Antenna. Nachrichtentechn. Vol. 23, 1970, pp. 74 - 79.

6. Niedermair, G. Dielectric Spherical Antenna. Dissertation: TU Munich, 1971.